FTUV-13-0606 IFIC-13-27 KA-TP-13-2013 LPN13-034 SFB/CPP-13-38 TTK-13-16

Higgs boson production in association with three jets via gluon fusion at the LHC: Gluonic contributions

Francisco Campanario[1,2,*] and Michael Kubocz[1,3,†]

[1] *Institute for Theoretical Physics, KIT, 76128 Karlsruhe, Germany.*
[2] *Theory Division, IFIC, University of Valencia-CSIC, E-46100 Paterna, Valencia, Spain*
[3] *Institut für Theoretische Teilchenphysik und Kosmologie, RWTH Aachen University, D52056 Aachen, Germany*

Higgs production in association with three jets via gluon fusion (GF) is an important channel for the measurement of the $\mathcal{CP}$-properties of the Higgs particle at the LHC. In this letter, we go beyond the heavy top effective theory approximation and include at LO the full mass dependence of the top- and bottom-quark contributions. We consider the dominant sub-channel $gg \to Hggg$ which involves the manipulation of massive rank-5 hexagon integrals. Furthermore, we present results for several differential distributions and show deviations from the effective theory as large as 100% at high p_T for light Higgs masses.

PACS numbers: 12.38.Bx, 13.85.-t, 14.65.Fy, 14.65.Ha, 14.70.Dj, 14.80.Bn

I. INTRODUCTION

Higgs production in association with two jets via gluon fusion is known to be an important channel at the LHC in order to measure the $\mathcal{CP}$-properties of the new found scalar particle. Indeed, the differential distribution of the azimuthal angle between the more forward and the more backward of the two tagging jets, $\phi_{jj} = \phi_{jF} - \phi_{jB}$, provides a sensitive probe for the $\mathcal{CP}$-character of the Higgs couplings to quarks [1–5]. A further aspect of interest is the modification of the azimuthal angle correlation by emission of additional jets, that is, at least by a third jet. Former investigations with showering and hadronization provided a strong de-correlation between the tagging jets in Higgs plus two jet production [6]. The de-correlation effects, however, were disproportionately illustrated due to approximations in the parton-shower. Further analyses [7–9] also showed, that after the separation of the hard radiation from the showering effects with subsequent hadronization, the ϕ_{jj}-correlation survives with minimal modifications. Similar results were obtained by a parton level calculation with NLO corrections [10] to the Higgs plus two jets process in the framework of an effective Lagrangian. In this letter, we provide results for the sub-process $gg \to Hggg$ going beyond the heavy top approximation, including the full mass dependence of the top- and bottom-quark contributions at LO. This sub-process involves the manipulation of massive rank-5 hexagon Feynman diagrams, which are the most complicated topologies appearing in Higgs production in association with three jets via GF, and thus it provides a testing ground to check the numerical stability of the full process. This is particularly important for the numerically challenging bottom-loop corrections, which are small within the SM, however, once a $\mathcal{CP}$-odd Higgs is considered, large corrections can arise for large values of $\tan\beta$, which can be used to discriminate the $\mathcal{CP}$-properties of the new found scalar particle– a pure $\mathcal{CP}$-odd scalar Higgs has been already discarded with more than three standard deviations [11], however, a $\mathcal{CP}$-violating Higgs boson consisting of a mixture of $\mathcal{CP}$-odd and $\mathcal{CP}$-even couplings to fermions, is still not. Within the SM, $gg \to Hggg$ is the dominant channel, hence, an essential piece to compute the real emission contributions for Higgs plus two jets production at NLO via GF. Results for the full process and a detailed description of de-correlation effects will be given in a forthcoming publication. Furthermore, the presented results are important to study the validity of the effective Lagrangian approach in Higgs production plus two and three jets. They are also relevant for heavy-Higgs searches beyond the Standard Model, since large deviations with respect to the effective theory are expected for a Higgs mass, m_H, bigger than twice the top-quark mass, m_t.

This letter is organized as follows: in Section II, the details of the calculations are given. Numerical results are presented in Section III. Finally, we summarize in Section IV.

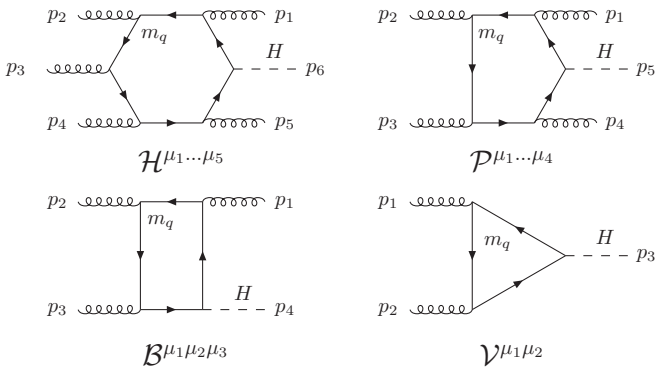

FIG. 1: Master Feynman diagrams

* francisco.campanario@ific.uv.es
† kubocz@physik.rwth-aachen.de

II. CALCULATION

The production of the $\mathcal{CP}$-even Higgs boson H at order α_s^5 can be carried out via the following sub-processes (+ crossing related) [12]:

$$q\,q \to q\,q\,g\,H, \quad q\,Q \to q\,Q\,g\,H,$$
$$q\,g \to q\,g\,g\,H, \quad g\;g \to g\,g\,g\,H\,. \tag{1}$$

In this letter, we restrict our analysis to the last sub-channel containing only gluons in the initial and final state. We use the effective current approach [13, 14], which allows us to compute only four master Feynman diagrams, depicted in Fig. 1. Note that the attached gluons are treated generally as off-shell vector currents. The calculation of the master integrals is performed with the in-house framework described in Ref. [15]. Additionally, we reduce the number of diagrams to be computed applying the Fury's theorem to all contributing topologies. Based on the gluon fusion part *GGFLO* of the program *VBFNLO* [16], we devote special care to the development of a fully-flexible, numerically stable parton-level Monte Carlo program. The control of numerical instabilities, appearing in each of the master diagrams due to vanishing Gram determinants, is done evaluating Ward identities, which replace the polarization vectors of attached gluons by their corresponding momenta. This allows us to relate and additionally check the master Feynman diagrams depicted in Fig. 1. For example, a hexagon topology of rank five is written as a difference of two pentagons topologies of rank four

$$\mathcal{H}^{\mu_1\cdots\mu_5} p_{i,\mu_i} = \mathcal{P}_1^{\mu_1\cdots\hat{\mu}_i\cdots\mu_5} - \mathcal{P}_2^{\mu_1\cdots\hat{\mu}_i\cdots\mu_5},\; i = 1\ldots 5\,, \tag{2}$$

where $\hat{\mu}_i$ denotes the corresponding vertex replaced by its momentum p_i. We construct all possible Ward identities for each physical permutation and diagram, e.g. all five different ones for the hexagon $\mathcal{H}^{\mu_1\cdots\mu_5}$. These Ward identities are evaluated for each phase space point and diagram with a small additional computing cost using a cache system. If the identities are not satisfied better than five per ten thousand level for a given diagram, this one is reevaluated by computing the scalar integrals and tensor reduction routines in quadruple precision. The complete phase-space point is rejected and the amplitude set to zero if the Ward Identities are not satisfied after this step. With this system, we find that the amount of phase-space points, which does not pass the Ward identities for a requested accuracy of $\epsilon = 5 \times 10^{-4}$, is statistically negligible and well below the per mille level, taking into account also the numerically challenging bottom-loop contributions (5% of the phase space points are rejected when using only double precision). This method was also applied successfully in ZZ+jet production via GF in Ref. [17]. Final results are given demanding a global accuracy of the Ward identities of $\epsilon = 5 \times 10^{-4}$. For the numerical evaluation of tensor integrals, we apply the Passarino-Veltman approach of Ref. [18] up to boxes, and for a numerically stable implementation of five-point-coefficients, we use the scheme laid out in Ref. [15]. Corresponding color factors were computed by hand and cross-checked with the program MADGRAPH [19, 20]. To define a color basis, it is strategically favorable to start with hexagons and investigate their color structure. The five external gluons give rise to $5! = 120$ hexagons (60 after applying Fury's theorem) proportional to color traces of the form

$$\mathrm{tr}\left[t^{a_i}t^{a_j}t^{a_k}t^{a_l}t^{a_m}\right] \quad \text{with} \quad i,j,k,l,m = 1,\ldots,5 \quad \text{and} \quad i \neq j \neq k \neq l \neq m\,, \tag{3}$$

in which $(5-1)! = 24$ are independent of each other. Thus, they can be used to form a color basis for all remaining amplitudes with triangle-, box- and pentagon-like topologies.

To cross check our results, we have compared the top-loop contribution with the heavy top-mass approximation, which is also a part of the GF-implementation within the VBFNLO framework. The agreement at the integrated cross section level for $m_t = 5 \cdot 10^4$ GeV is better than one per ten thousand. We have also performed a comparison with Madgraph and got agreement at the per mille level. Additionally, gauge invariance was checked at the amplitude level with expected cancellations of the order of the machine precision.

III. NUMERICAL RESULTS

In this section, we present integrated cross sections and differential distributions for the sub-process $gg \to gggH$ at the LHC for various center of mass (c.o.m.) energies. The Higgs boson is produced on shell and without finite width effects. We set the top-quark mass to $m_t = 173.3\,\mathrm{GeV}$, the $\overline{\mathrm{MS}}$ bottom-quark mass to $\overline{m}_b(m_b) = 4.2\,\mathrm{GeV}$, and the other light quark masses to zero. Within the Higgs-mass range of 100-600 GeV, the bottom-quark mass is 33-42% smaller than the pole mass of 4.855 GeV used in the loop propagators. Thus, we take into account the evolution of m_b up to a reference scale, here m_H, and the relation between the pole mass and the $\overline{\mathrm{MS}}$ mass. Additionally, we choose $M_Z = 91.188\mathrm{GeV}$, $M_W = 80.386\mathrm{GeV}$ and $G_F = 1.16637 \times 10^{-5}\mathrm{GeV}^{-2}$ as electroweak input parameters and derive further necessary parameters from Standard Model tree level relations. Cross section predictions are obtained using the CTEQ6L1 parton distribution functions (PDFs) [21] with the default strong coupling value $\alpha_s(M_Z) = 0.130$. The factorization scale is set to $\mu_F = (p_T^{j1} p_T^{j2} p_T^{j3})^{1/3}$ and the renormalization to

$$\alpha_s^5(\mu_R) = \alpha_s(p_T^{j_1})\alpha_s(p_T^{j_2})\alpha_s(p_T^{j_3})\alpha_s(p_H)^2\,. \tag{4}$$

Here, $p_T^{j_i}$ with $i = 1,2,3$ denotes jets with decreasing transverse momenta. We use the k_T jet algorithm and impose

$$p_T^{j_i} > 20\ \mathrm{GeV}\,, \qquad |\eta_j| < 4.5\,, \qquad R_{jj} > 0.6\,, \tag{5}$$

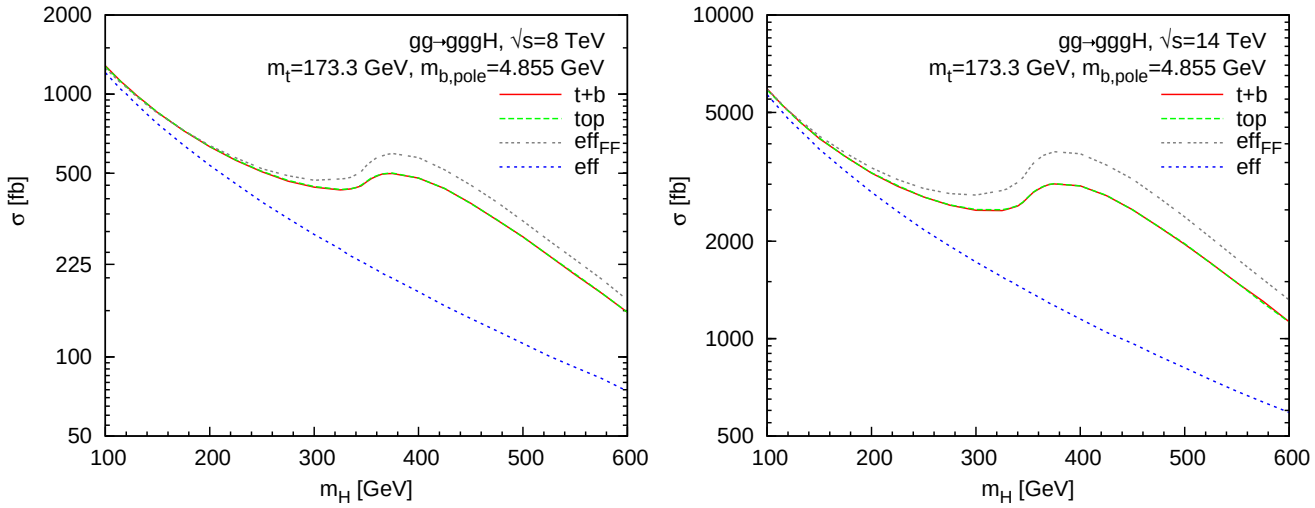

FIG. 2: Cross section of the $gg \to gggH$ scattering sub-process as a function of Higgs boson mass for c.o.m. energies of 8 TeV and 14 TeV. Both panels show the effective theory (with and without FF) and full mass contributions. The inclusive cuts (IC) of Eq. (5) have been applied.

m_H	σ[fb] / $\sqrt{s}$	7 TeV	8 TeV	14 TeV
126 GeV	σ(t)	674.7 ± 0.3	1017 ± 0.5	4846 ± 1
	σ(t+b)	676 ± 0.4	1019 ± 0.5	4864 ± 1
400 GeV	σ(t)	292.9 ± 0.2	480.2 ± 0.3	2965 ± 0.8
	σ(t+b)	292.6 ± 0.2	480.1 ± 0.3	2962 ± 1

TABLE I: Cross sections evaluated for different Higgs masses and c.o.m. energies applying the inclusive set of cuts (IC) of Eq. (5).

where R_{jj} describes the separation of the two partons in the pseudo-rapidity versus azimuthal-angle plane,

$$R_{jj} = \sqrt{\Delta\eta_{jj}^2 + \phi_{jj}^2}\,, \tag{6}$$

with $\Delta\eta_{jj} = |\eta_{j1} - \eta_{j2}|$ and $\phi_{jj} = \phi_{j1} - \phi_{j2}$. These cuts anticipate LHC detector capabilities and jet finding algorithms and will be called "inclusive cuts" (IC). Values of cross sections for two different Higgs masses evaluated at different c.o.m. energies are summarized in table I. A Higgs mass of 400 GeV has been chosen to show maximal deviations of the effective theory approximation for Higgs masses larger than $2m_t$ despite of the experimental SM Higgs boson exclusion limits. As expected, bottom-loop corrections hardly contribute to the overall cross section, and hence, they can be neglected within the SM framework. Noticeable is the negative impact of the interference term between top- and bottom-loop induced contributions for a Higgs mass of 400 GeV, which decreases the overall cross section by a small amount.
The total cross section as a function of the Higgs boson mass is shown in Fig. 2 for c.o.m. energies of 8 TeV (left panel) and 14 TeV (right panel). Amplitudes with a top-loop mediated contribution give rise to a striking peak due to the threshold enhancement around $m_H \approx 2m_t$. Here, we removed the singular behavior at $m_H = 2m_t$ by omitting the corresponding phase-space point. For the effective theory approximation, we used two approaches: pure effective Higgs coupling to fermions in the heavy top-quark limit with and without corrections by an additional form factor (FF) [22]. Up to Higgs masses of 150 (175) GeV (within 10 % deviation with respect to the full theory), the effective theory approximation gives accurate results for a c.o.m. energy of 8 (14) TeV. The application of the form factor FF extends additionally the validity range of the effective approximation to higher Higgs masses, here up to 330 GeV for $\sqrt{s} = 8$ TeV (within 10% deviation with respect to the full theory), whereas for $\sqrt{s} = 14$ TeV the upper validity bound is fixed at 290 GeV. Furthermore, it gives back the top-quark mass dependence imitating the threshold enhancement of the full theory. Beyond the validity bound, the total cross section is overestimated up to 20 (25)% for 8 (14) TeV c.o.m. energy at $m_H = 400$ GeV, and converges afterwards slowly to the full theory result for the shown range of Higgs mass.

Next, for a c.o.m. energy of 14 TeV, we present some differential distributions for Higgs masses of 126 GeV (left panels) and 400 GeV (right panels). Presented results were evaluated with contributions mediated by quark-loops, $(t + b)$, and with the effective theory framework including form factor corrections, eff_{FF}. Differences between both approaches are illustrated with the help of a K-factor defined as $\text{eff}_{\text{FF}}/(t + b)$. The differential distributions for the hardest jet are shown in Fig. 3. In the left panel, one can see that the effective theory provides, as expected, a very good approximation of the full theory up to $p_T^{\text{jmax}} < 200$ GeV.

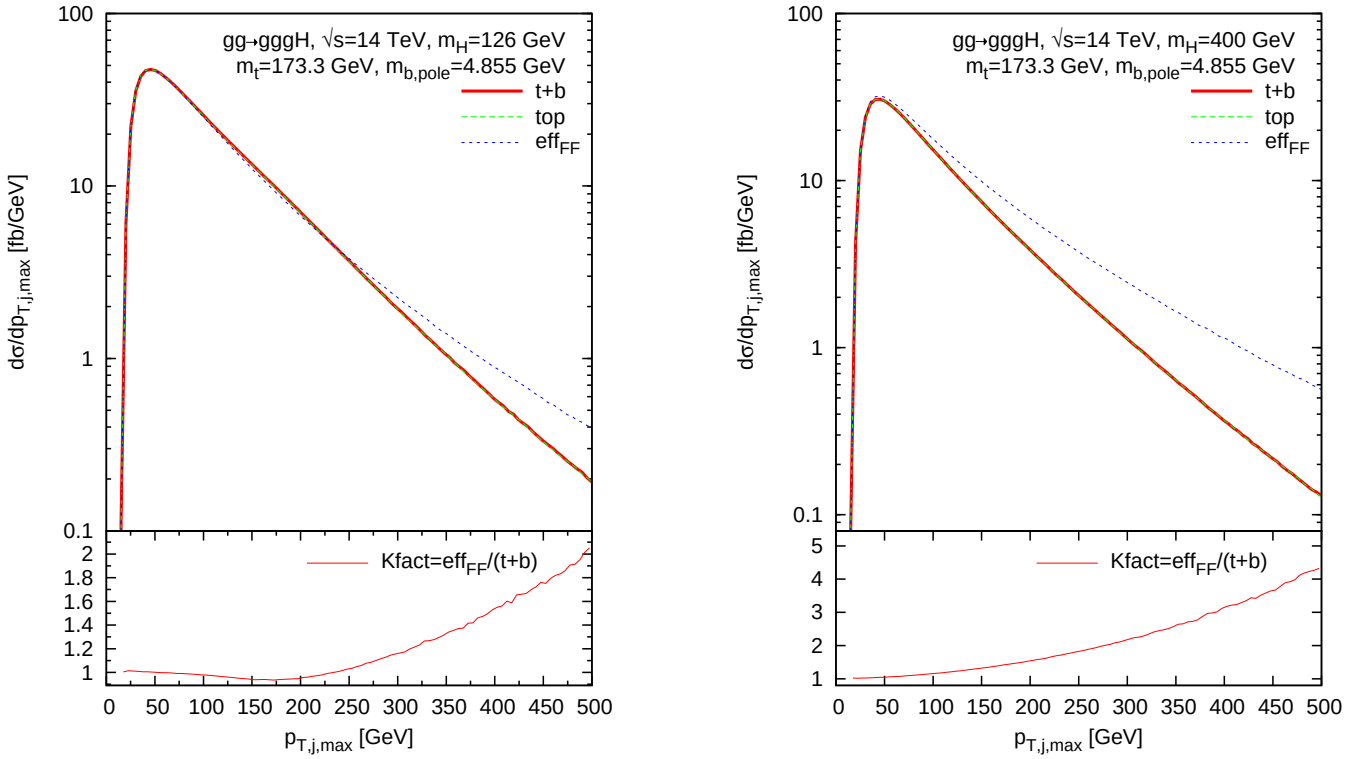

FIG. 3: Comparison of transverse-momentum distributions of the harder jet of the $gg \to gggH$ scattering sub-process evaluated within the effective and loop-induced theory. The inclusive cuts (IC) of Eq. (5) are applied.

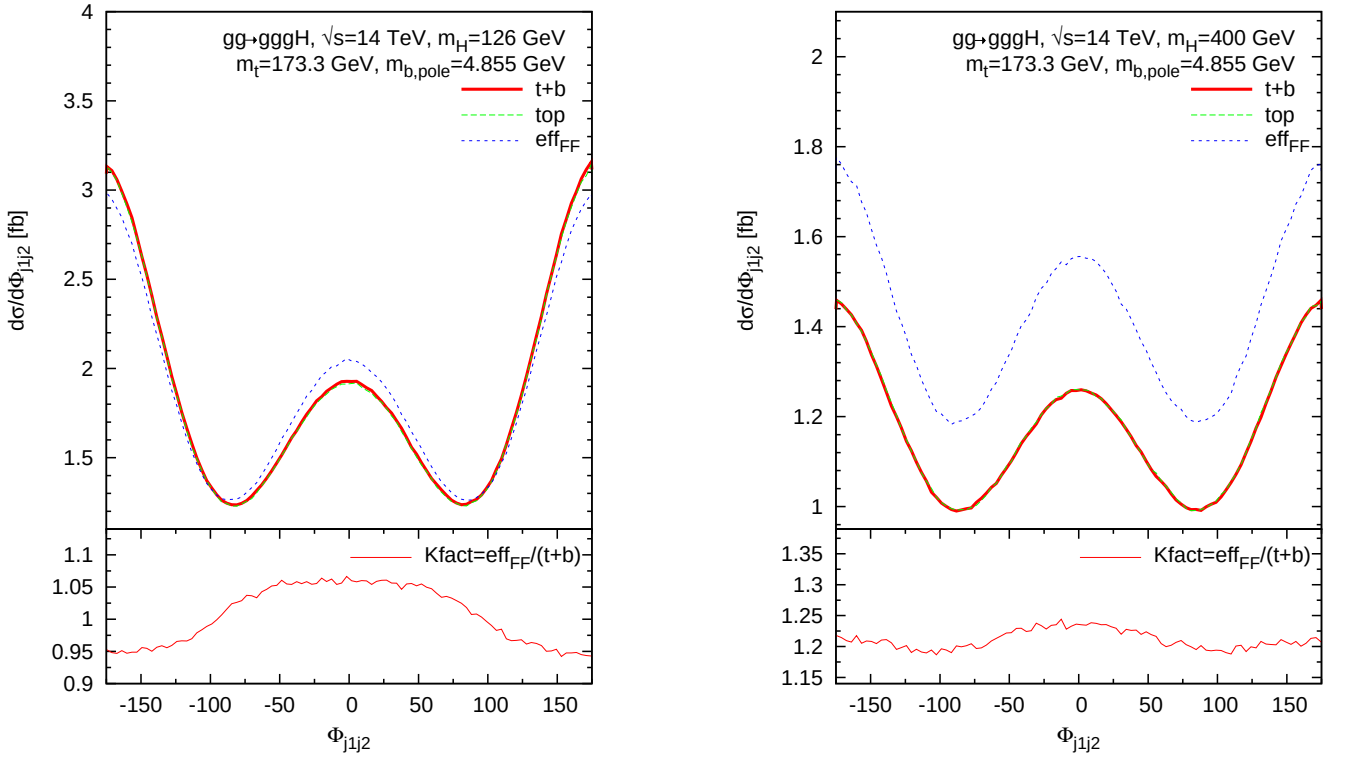

FIG. 4: Comparison of azimuthal angle distributions of the $gg \to gggH$ scattering sub-process evaluated within the effective and loop-induced theory. The ICphi set of acceptance cuts of Eq. (7) is applied.

Beyond that regime, differences start to increase and deviations up to 100% are found. The discrepancy of the differential distribution illustrated in the right panel are more evident. At the maximum of the differential distribution, the deviation of the effective theory is only about 5%. As the p_T increases, the effective theory predicts harder emissions, which are overestimated up to a factor of 5 and add to the total 25% discrepancy at the level of the total cross section.

Following the definition of Ref. [2], the azimuthal angle distributions between the more forward and the more backward of the two tagging jets are depicted in Fig. 4. The calculation was carried out with a modified set of cuts, which leads to a better sensitivity to the $\mathcal{CP}$-structure of the Higgs couplings than the inclusive cuts. We use

$$p_T^{j_i} > 30 \text{ GeV} \, , \; |\eta_j| < 4.5 \, , \; R_{jj} > 0.6 \, , \; \Delta\eta_{jj} > 3 \, , \quad (7)$$

and label it as the ICphi set of cuts in the following.

The effective theory approximation provides a good description in the whole azimuthal angle range with a deviation up to the 5% level for a 126 GeV massive Higgs boson. For a 400 GeV Higgs boson mass, the shape is well reproduced, but 20 % off in the whole spectrum.

IV. SUMMARY

We have presented a short analysis of the gluon fusion loop-induced sub-process $gg \to gggH$ at the LHC, which is the dominant one in Higgs production in association with three jets via GF. We devoted special attention to the development of a numerical stable MC program which solves the problem of vanishing Gram determinants by suitable application of Ward identities and quadruple precision. We have also included bottom-loop corrections, although they are negligible in the SM framework, to show additionally the numerical stability of the contributing integrals for small loop-masses (they will become relevant in combination with a $\mathcal{CP}$-odd Higgs boson and large $\tan\beta$ values). Up to Higgs masses of 290 GeV for $\sqrt{s} = 14$ TeV (330 GeV @ 8 TeV) and for small transverse momenta $p_T^{j\max} \lesssim 290$ GeV, the effective Lagrangian approximation with the form factor correction gives accurate results and can be used as a numerically fast alternative for phenomenological studies. No restriction was found in the validity of the invariant mass of the dijet system of the leading jets (not shown). For a 400 GeV Higgs mass, large deviation can be found for small transverse momenta $p_T^{j\max} \lesssim m_t$. Furthermore, the azimuthal angle distribution, sensitive to the $\mathcal{CP}$-property measurements, is (relatively) well described by the effective theory both in shape and normalization for (heavy) light Higgs masses. A detailed description of the full process and de-correlation effects will be given in a forthcoming publication. This process will be made publicly available as part of the VBFNLO program.

ACKNOWLEDGMENTS

It is a pleasure to thank Dieter Zeppenfeld for fruitful discussions during the development of this project. We acknowledge the support from the Deutsche Forschungsgemeinschaft via the Sonderforschungsbereich/Transregio SFB/TR-9 Computational Particle Physics. FC is funded by a Marie Curie fellowship (PIEF-GA-2011-298960) and partially by MINECO (FPA2011-23596) and by LHCPhenonet (PITN-GA-2010-264564) and acknowledges the Institute for Theoretical Physics, at KIT for the use of the computer Grid Cluster. MK acknowledge support by the Grid Cluster of the RWTH-Aachen.

[1] T. Plehn, D. L. Rainwater, and D. Zeppenfeld, Phys.Rev.Lett. **88**, 051801 (2002), hep-ph/0105325.
[2] V. Hankele, G. Klamke, D. Zeppenfeld, and T. Figy, Phys.Rev. **D74**, 095001 (2006), hep-ph/0609075.
[3] G. Klamke and D. Zeppenfeld, JHEP **0704**, 052 (2007).
[4] K. Hagiwara, Q. Li, and K. Mawatari, JHEP **0907**, 101 (2009), 0905.4314.
[5] F. Campanario, M. Kubocz, and D. Zeppenfeld, Phys.Rev. **D84**, 095025 (2011), 1011.3819.
[6] K. Odagiri, JHEP **0303**, 009 (2003), hep-ph/0212215.
[7] V. Del Duca *et al.*, JHEP **0610**, 016 (2006).
[8] V. Del Duca, Acta Phys.Polon. **B39**, 1549 (2008).
[9] J. R. Andersen, K. Arnold, and D. Zeppenfeld, JHEP **1006**, 091 (2010), 1001.3822.
[10] J. M. Campbell, R. K. Ellis, and G. Zanderighi, JHEP **0610**, 028 (2006), hep-ph/0608194.
[11] A. Freitas and P. Schwaller, Phys.Rev. **D87**, 055014 (2013), 1211.1980.
[12] M. Kubocz, *Higgs production via gluon fusion in association with two or three jets in supersymmetric models*, PhD thesis, Karlsruhe Institute of Technology (KIT), 2009, digbib.ubka.uni-karlsruhe.de/volltexte/documents/1379672.
[13] K. Hagiwara and D. Zeppenfeld, Nucl.Phys. **B274**, 1 (1986).
[14] K. Hagiwara and D. Zeppenfeld, Nucl.Phys. **B313**, 560 (1989).
[15] F. Campanario, JHEP **1110**, 070 (2011), 1105.0920.
[16] K. Arnold *et al.*, Comput.Phys.Commun. **180**, 1661 (2009), 0811.4559.
[17] F. Campanario, Q. Li, M. Rauch, and M. Spira, (2012), 1211.5429.
[18] G. Passarino and M. Veltman, Nucl.Phys. **B160**, 151 (1979).
[19] J. Alwall *et al.*, JHEP **0709**, 028 (2007), 0706.2334.
[20] J. Alwall, M. Herquet, F. Maltoni, O. Mattelaer, and T. Stelzer, JHEP **1106**, 128 (2011), 1106.0522.
[21] J. Pumplin *et al.*, JHEP **0207**, 012 (2002).
[22] A. Djouadi, Phys.Rept. **457**, 1 (2008), hep-ph/0503172.